Influence of Localized Umklapp Scattering on the Galvanomagnetic Properties of Metals*

RICHARD A. YOUNG†‡
Department of Physics and James Franck Institute, University of Chicago, Chicago, Illinois 60637
(Received 3 July 1968)

The Boltzmann equation is used to investigate the influence of umklapp scattering on the galvanomagnetic properties of a nearly-free-electron bcc metal with a spherical Fermi surface. A phenomenological scattering function is used to describe the umklapp scattering. If the areas of the Fermi surface where umklapp scattering occurs are very small and the scattering very intense, the transverse magnetoresistance is found to increase linearly with the magnetic field to a saturation value. The linear variation can occur up to values of $\omega_c\tau$ as large as 150, i.e., well into the high-magnetic-field region. The Hall "constant" is also found to vary with the magnetic field strength. Application of the results to potassium, aluminum, and cadmium is briefly discussed.

I. INTRODUCTION

THE possibility of obtaining information about the electronic structure of a metal from its galvanomagnetic properties was first proposed theoretically in a rigorous fashion by Lifshitz, Azbel, and Kaganov (LAK).[1] The LAK theory was first applied to specific physical situations by Lifshitz and Peschanskii.[2] The LAK theory, together with the work of Lifshitz and Peschanskii, provided an interpretation for much of the previously unexplained behavior of the magnetoresistance of metals.[3,4] The main feature of the LAK theory is its emphasis in the geometry of $\mathbf{k}$ space and its disregard of the exact nature of the scattering process. The most significant results are summarized in Table I. A further important result of the LAK theory is its agreement with Kohler's rule, which states that

$$\Delta\rho/\rho(0)=[\rho(\mathbf{H})-\rho(0)]/\rho(0)$$

is a function only of $|\mathbf{H}|[\rho(0)]^{-1}$. However, the agreement with Kohler's rule is valid only if magnetic breakdown[5] is not present and if the sole effect of a change in temperature or purity of the sample may be described by changing τ to $\lambda\tau$, where λ is a constant and τ is a relaxation time which can be used to describe the scattering process.

In spite of the success of the LAK theory there remains a number of metals (e.g., potassium, copper, silver, and aluminum) whose galvanomagnetic properties do not agree with those predicted by the LAK theory.[3,4,6] In particular, recent experiments which measure the transverse magnetoresistance of potassium[7–9] indicate that the scattering mechanism can play as important a role in determining the high-magnetic-field behavior of the resistivity tensor as does the geometry of the orbit in the LAK theory. Since the Fermi surface of potassium[10] may be considered to be spherical to one part in 10^3, the theory of LAK predicts that the transverse magnetoresistance should saturate at high magnetic fields. Also, since the Fermi surface is contained within the first Brillouin zone there can be no magnetic breakdown effects present. Penz[8,9] finds that the transverse magnetoresistance increases linearly with magnetic field for values of $\omega_c\tau$ as large as 150, where ω_c is the cyclotron frequency and τ is a relaxation time determined from the dc resistance of the single crystal. The transverse magnetoresistance exhibits some correlation with the orientation of the magnetic field relative to the crystal axes and with the amount of stress exerted on the sample.[11] Finally, we note that these results show a marked deviation from Kohler's rule.

Further evidence of the influence of scattering on the behavior of the galvanomagnetic properties has been found in cadmium[12] and in aluminum.[13–16] Both the

* Research supported in part by the U. S. Office of Naval Research and the National Science Foundation.

† Submitted in partial fulfillment of the requirements for the Ph.D. degree at the University of Chicago.

‡ Present address: Department of Physics, University of Arizona, Tucson, Arizona.

[1] I. M. Lifshitz, M. Ya. Azbel, and M. I. Kaganov, Zh. Eksperim. i Teor. Fiz. **30**, 220 (1955); **31**, 63 (1956) [English transls.: Soviet Phys.—JETP **3**, 143 (1956); **4**, 41 (1957)].

[2] I. M. Lifshitz and V. G. Peschanskii, Zh. Eksperim. i Teor. Fiz. **35**, 1251 (1958); **38**, 188 (1960) [English transls.: Soviet Phys.—JETP **8**, 875 (1959); **11**, 137 (1960)].

[3] E. Fawcett, Advan. Phys. **13**, 139 (1964), and references therein.

[4] R. G. Chambers, in *The Fermi Surface*, edited by W. A. Harrison and M. B. Webb (John Wiley & Sons, Inc., New York, 1962), p. 100 and references therein.

[5] R. W. Stark and L. M. Failcov in *Progress in Low Temperature Physics*, edited by C. J. Gorter (North-Holland Publishing Co., Amsterdam, 1967), p. 235 and references therein.

[6] A. B. Pippard, *Proceedings of the Alta Lake Summer School on Electrons in Metals, British Columbia, 1967* (Gordon and Breach Science Publishers, Inc., 1968).

[7] F. E. Rose, Ph.D. thesis, Cornell University, 1964 (unpublished).

[8] P. A. Penz, Ph.D. thesis, Cornell University, 1967 (unpublished).

[9] A. Penz and R. Bowers, Solid State Commun. **5**, 341 (1967).

[10] D. Shoenberg and P. J. Stiles, Proc. Roy. Soc. (London) **A281**, 62 (1964).

[11] P. A. Penz and R. Bowers, Phys. Rev. **172**, 991 (1968).

[12] D. C. Tsui and R. W. Stark, Phys. Rev. Letters **19**, 1317 (1967); C. G. Grenier, K. R. Efferson, and J. M. Reynolds, Phys. Rev. **143**, 406 (1966); and H. J. Mackey, J. R. Sybert, and J. T. Fielder, *ibid.* **157**, 578 (1967).

[13] V. G. Volotskaya, Zh. Eksperim. i Teor. Fiz. **44**, 80 (1963) [English transl.: Soviet Phys.—JETP **17**, 56 (1963)].

[14] R. J. Balcombe, Proc. Roy. Soc. (London) **A275**, 113 (1963).

[15] E. S. Borovik, V. G. Volotskaya, and N. Ya. Fogel, Zh. Eksperim. i Teor. Fiz. **45**, 46 (1963) [English transl.: Soviet Phys.—JETP **18**, 34 (1964)].

[16] E. S. Borovik and V. G. Volotskaya, Zh. Eksperim. i Teor. Fiz. **48**, 1554 (1965) [English transl.: Soviet Phys.—JETP, **21**, 1041 (1965)].

TABLE I. Magnetic-field dependence of the galvanomagnetic properties of metals in the high-field limit.

Type of orbits and state of compensation	Transverse magneto-resistance	Transverse Hall voltage
I. All closed orbits Uncompensated $n_e \neq n_h$	Saturates	$H/(n_e-n_h)$
II. All closed orbits Compensated $n_e=n_h$	H^2	H
III. Open in direction perpendicular to H and making angle α with current	$H^2\cos^2\alpha$	H

experiments on aluminum and cadmium indicate that Kohler's rule is violated in the high-magnetic-field region.

The variation of ρ_{21} with magnetic field strength ($\mathbf{H}\|[0001]$) shows a most unusual behavior in the case of cadmium. Since cadmium is a compensated metal it is difficult to predict what the sign of the Hall resistivity should be. One would expect, however, that in the high-field limit the sign of the Hall coefficient would not change as the temperature of a cadmium sample is varied. The experimental results, however, indicate that the sign of the Hall resistivity changes as the temperature of the sample increases from 2 to 4°K, the sign being negative (electronlike) at 2°K and positive (holelike) at 4°K. The existing theory of high-magnetic-field galvanomagnetic properties (LAK with magnetic breakdown) is incapable of explaining the unusual behavior of the Hall resistivity in cadmium.

From the above examples it is obvious that a careful study of the effect of scattering on the behavior of the magnetoresistance is needed. Both Pippard[5,17] and Jones and Sondheimer[18] have considered the explicit dependence of the magnetoresistance on the scattering of the electrons. Neither of these papers, however, makes any attempt to include the explicit effects of umklapp scattering on the electrons.

In this paper we investigate the effects of umklapp scattering on the behavior of the galvanomagnetic properties of a nearly-free-electron metal. The umklapp scattering is treated by using a phenomenological scattering function and explicitly including the effects of such a scattering function in the solution of the Boltzmann equation. Since our primary interest is in the influence of scattering, we shall consider only a single-sheet spherical Fermi surface (such a surface shows no magnetoresistance in the relaxation time approximation) which is close enough to the Brillouin zone boundaries to allow an appreciable amount of wave-function mixing for wave vectors $\mathbf{k}$ which are in the immediate neighborhood of the zone faces. Such wave-function mixing can give rise to umklapp scattering which, under extreme conditions, can generate electron

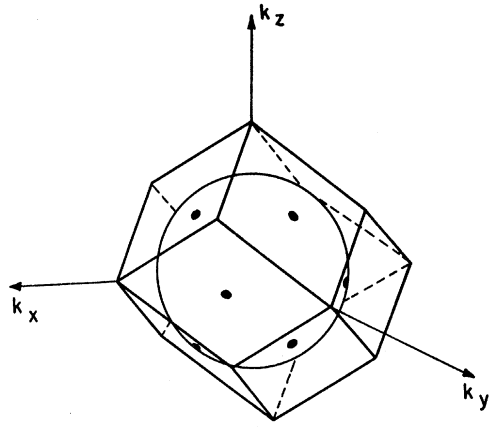

FIG. 1. A spherical Fermi surface enclosed by the first Brillouin zone of a bcc lattice. The shaded regions indicate the areas of the Fermi surface where large-angle (hot spot) scattering can occur.

trajectories in $\mathbf{k}$ space which closely resemble those that would occur if magnetic breakdown were present. The effect, however, as shown in Sec. II is opposite to that of magnetic breakdown in the sense that it becomes less pronounced as $|\mathbf{H}|$ increases. In Sec. II we define the model of the Fermi surface and the scattering function of the electrons to be used in our calculation. In Sec. III the linearized Boltzmann equation is solved for the above model and the resistivity tensor is determined. In Sec. IV the results of the above calculation are analyzed for various cases which may be of physical interest.

II. SCATTERING MODEL

We consider a nearly-free-electron metal with a bcc lattice and a spherical Fermi surface lying entirely within the first Brillouin zone (Fig. 1). We assume that the one-electron wave function $\psi_{\mathbf{k}}$ for a wave vector $\mathbf{k}$ lying on the Fermi surface ($|\mathbf{k}|=k_F$) may be written as a linear combination of the two plane waves $|\mathbf{k}\rangle$ and $|\mathbf{k}-\mathbf{K}_i\rangle$, where

$$|\mathbf{k}\rangle=\Omega^{-1/2}\exp(i\mathbf{k}\cdot\mathbf{r}). \tag{2.1}$$

Here Ω is the volume of the crystal and $\mathbf{K}_i$ is one of the 12 reciprocal lattice vectors whose normal planes define the first Brillouin zone of the bcc lattice.[19] Thus the wave function for the state $\mathbf{k}$ assumes the form

$$\psi_{\mathbf{k}}=a_1(\mathbf{k})|\mathbf{k}\rangle+a_2(\mathbf{k})|\mathbf{k}-\mathbf{K}_i\rangle. \tag{2.2}$$

The proper $\mathbf{K}_i$ to be inserted into Eq. (2.2) is the one which minimizes $\mathbf{k}\cdot\mathbf{K}_i$.

One consequence of the plane-wave mixing given by by Eq. (2.2) is illustrated by the calculation of the matrix element $\langle\psi_{\mathbf{k}'}|V|\psi_{\mathbf{k}}\rangle$, where V is a perturbing potential to the otherwise perfect crystal lattice. The

[17] A. B. Pippard, Proc. Roy. Soc. (London) **A282**, 464 (1964).
[18] M. C. Jones and E. H. Sondheimer, Phys. Rev. **155**, 567 (1967), hereafter referred to as JS.

[19] For a more complete discussion of this approximation see J. G. Collins, Proc. Roy. Soc. (London) **A263**, 531 (1961).

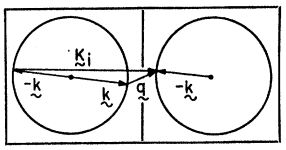

FIG. 2. A typical large-angle scattering event ($\mathbf{k} \rightarrow -\mathbf{k}$) for a small $|\mathbf{q}|$ due to plane-wave mixing.

use of (2.2) for $\psi_{\mathbf{k}}$ and $\psi_{\mathbf{k}'}$ yields, in the case $\mathbf{k}'=-\mathbf{k}$,

$$\langle\psi_{-\mathbf{k}}|V|\psi_{\mathbf{k}}\rangle = a_1^*(-\mathbf{k})a_1(\mathbf{k})V_{2\mathbf{k}} + [a_2^*(-\mathbf{k})a_1(\mathbf{k}) + a_2(\mathbf{k})a_1^*(-\mathbf{k})]V_{\mathbf{K}_i-2\mathbf{k}} + a_2(\mathbf{k})a_2^*(-\mathbf{k})V_{2\mathbf{K}_i-2\mathbf{k}}, \quad (2.3)$$

where we set $V_{\mathbf{q}}=\langle\mathbf{k}+\mathbf{q}|V|\mathbf{k}\rangle$ and we have assumed that $V_{\mathbf{q}}$ is a function of $|\mathbf{q}|$ only. Equation (2.3) shows that even if $V_{\mathbf{q}}=0$ for large angle scattering, i.e., for $|\mathbf{q}|$ larger than some q_0, we can still get large-angle scattering (umklapp scattering) if $|\mathbf{K}_i-2\mathbf{k}|\leq q_0$. Thus a potential whose $V_{\mathbf{q}}$ is sharply peaked at $|\mathbf{q}|=0$ and which would normally give rise only to small-angle scattering (i.e., $q_0 \ll 2k_F$) produces large-angle scattering as a result of the plane-wave mixing given by (2.2). One such scattering process is illustrated in Fig. 2.

Since $|a_2(\mathbf{k})|$ would normally decrease as $|\mathbf{k}\cdot\mathbf{K}_i|$ decreases, we will, as a first approximation, neglect the effects of wave-function mixing except when $\mathbf{k}$ is nearly antiparallel to some $\mathbf{K}_i$. We can then include phenomenologically the possibility of large-angle scattering by assuming that for a solid angle Ω_0 about all the $\mathbf{K}_i$'s we can get large-angle scattering. We shall call these angular regions *hot spots*. Outside of these hot-spot regions we assume that $|a_2(\mathbf{k})|$ can be considered negligible and as a consequence V gives rise only to small-angle scattering (Fig. 1). Eventually we must allow for the possibility that $|a_2(\mathbf{k})|$ is large enough to generate large-angle scattering over most of the Fermi surface; this is accomplished by letting Ω_0 increase. In all cases, regardless of the size of $|a_2(\mathbf{k})|$, we retain the spherical Fermi surface as a computational convenience.[20] It is important to notice that the hot-spot scattering as described above occurs only between two hot spots. Such scattering has a well-defined directional character which must be explicitly included in the calculation of the resistivity tensor.

In order to determine the scattering properties of these hot spots the following classical two-channel problem may be considered. We assume that there are two channels, A and B and a variable φ which specifies the position along the channels. On each channel we specify a function $S(\varphi_A,\varphi_B)=S(\varphi_B,\varphi_A)$ such that $S(\varphi_A,\varphi_B)d\varphi_A$ is the probability per unit time that a particle at φ_B will be scattered into the range between φ_A and $\varphi_A+d\varphi_A$. For convenience we assume that $S(\varphi_A,\varphi_B)$ is nonzero only in the region $0\leq\varphi_A,\ \varphi_B\leq\Delta$, and we neglect any intrachannel scattering.

[20] It is well known from energy-band calculations for the alkali metals that in spite of the mixing of plane waves the Fermi surface remains spherical for potassium. See, e.g., F. S. Ham, Phys. Rev. 128, 82 (1962).

The problem may then be stated as follows: If a particle enters channel A at time $t=0$, we must find the probability that the particle is in channel A at $t=\infty$. If we let $U_{A(B)}(\varphi_{A(B)},t)d\varphi_{A(B)}$ be the probability that the particle will be in channel $A(B)$ between $\varphi_{A(B)}$ and $\varphi_{A(B)}+d\varphi_{A(B)}$ at time t, and $\omega_c=d\varphi_A/dt=d\varphi_B/dt$ be the drift velocity of the particle on either channel, then the following system of integro-differential equations is obtained (for derivation see Appendix):

$$\omega_c\frac{\partial U_A}{\partial\varphi_A}+\frac{\partial U_A}{\partial t}=-U_A\int_0^\Delta d\varphi_B S(\varphi_B,\varphi_A) + \int_0^\Delta d\varphi_B U_B(\varphi_B,t)S(\varphi_A,\varphi_B), \quad (2.4)$$

$$\omega_c\frac{\partial U_B}{\partial\varphi_B}+\frac{\partial U_B}{\partial t}=-U_B\int_0^\Delta d\varphi_A S(\varphi_A,\varphi_B) + \int_0^\Delta d\varphi_A U_A(\varphi_A,t)S(\varphi_B,\varphi_A). \quad (2.5)$$

Equations (2.4) and (2.5) are to be solved with the boundary conditions

$$U_A(\varphi_A,0)=\delta(\varphi_A), \quad U_B(\varphi_B,0)=0, \quad (2.6)$$

where $\delta(x)$ is the Dirac δ function. Letting P be the probability that a particle will emerge in the incident channel, we have

$$P=\omega_c\int_0^\infty U_A(\Delta,t)dt \quad (2.7)$$

and

$$Q=\omega_c\int_0^\infty U_B(\Delta,t)dt=1-P, \quad (2.8)$$

where Q is the probability that the particle will emerge in the opposite channel.

The solution of (2.4) and (2.5) for P and Q for any separable scattering function $S(\varphi,\varphi')=s(\varphi)s(\varphi')$ is given in the Appendix. The result for the case $s(\varphi)=C^{1/2}(0\leq\varphi\leq\Delta)$, where C is a constant, is given by

$$P=\frac{1}{2}\left(1+\frac{e^{-1/\omega_c\mathcal{T}}-\frac{1}{2}\omega_c\mathcal{T}(1-e^{-1/\omega_c\mathcal{T}})}{1-\frac{1}{2}\omega_c\mathcal{T}(1-e^{-1/\omega_c\mathcal{T}})}\right); \quad (2.9)$$

$Q=1-P$, and we have set $\mathcal{T}^{-1}=C\Delta^2$. A graph of P and Q versus $\omega_c\mathcal{T}$ is shown in Fig. 3. The above formula is discussed in more detail in the appendix. For our present purposes it is only necessary to use the two limiting expressions for P and Q when $\omega_c\mathcal{T}\gg1$ and $\omega_c\mathcal{T}\ll1$. When $\omega_c\mathcal{T}\gg1$, we have $P\approx1-(\omega_c\mathcal{T})^{-1}$ and $Q\approx(\omega_c\mathcal{T})^{-1}$; when $\omega_c\mathcal{T}\ll1$, we can set $P\approx Q\approx\frac{1}{2}$. The first limit corresponds to the case where there is a very small probability of transfer between channels A and B as the particle passes through the scattering region; the second limit occurs when the particle is scattered many times

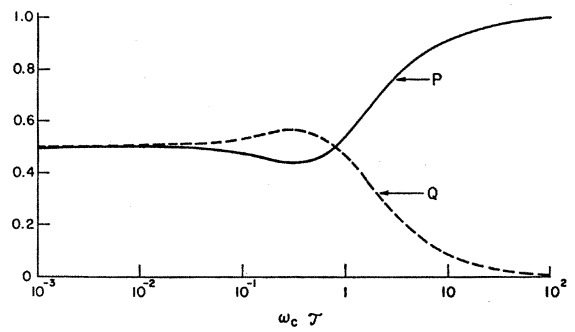

FIG. 3. Variation of P and Q as a function of $\omega_c\tau$ for $s(\varphi)=C^{1/2}$.

between channels A and B as it passes through the scattering region. The above asymptotic forms for P and Q are used in Sec. III to obtain a simple physical interpretation of the magnetoresistance of our model.

III. SOLUTION OF BOLTZMANN'S EQUATION

A. Relaxation Time Solution

In order to determine the effects of hot-spot scattering on the resistivity tensor we assume that the electron distribution function $f(\mathbf{k})$ satisfies the steady-state, spatially homogeneous Boltzmann equation, which we write as

$$\frac{1}{\hbar}\mathbf{F}\cdot\frac{df(\mathbf{k})}{d\mathbf{k}}=\int[f(\mathbf{k}')-f(\mathbf{k})]Q(\mathbf{k},\mathbf{k}')d\mathbf{k}'. \quad (3.1)$$

In (3.1) $\mathbf{F}$ is the external force acting on the electrons,

$$\mathbf{F}=\hbar\dot{\mathbf{k}}=-|e|[\mathbf{E}+(\mathbf{v}/c)\times\mathbf{H}], \quad (3.2)$$

and $Q(\mathbf{k},\mathbf{k}')d\mathbf{k}'$ is the transition probability per unit time that an electron with wave vector $\mathbf{k}$ will scatter to a state whose wave vector lies between $\mathbf{k}'$ and $\mathbf{k}'+d\mathbf{k}'$. Linearizing (3.1) in the electric field $\mathbf{E}$ and assuming that only elastic scattering can occur yields[21]

$$\mathbf{A}\cdot\mathbf{u}+\omega_c\frac{\partial g(\mathbf{k})}{\partial\varphi}=\int[g(\mathbf{k}')-g(\mathbf{k})]\mathcal{Q}(\mathbf{k},\mathbf{k}')d\Omega', \quad (3.3)$$

where $\mathbf{A}=\mathbf{E}/|\mathbf{E}|$, $\mathbf{u}=\mathbf{v}/v_F$, $\omega_c=|e||\mathbf{H}|/m^*c$, φ is the azimuthal angle of $\mathbf{k}$ about $\mathbf{H}$, and $\mathcal{Q}(\mathbf{k},\mathbf{k}')d\Omega'$ is the transition probability per unit time for an electron with wave vector $\mathbf{k}$ to be scattered into a solid angle $d\Omega'$ about $\mathbf{k}'$. The function $g(\mathbf{k})$ in (3.3) is defined by

$$f(\mathbf{k})=f_0+|e||\mathbf{E}||\mathbf{v}|(-\partial f_0/\partial\mathcal{E})g(\mathbf{k}), \quad (3.4)$$

where f_0 is the equilibrium Fermi distribution function. At very low temperatures $(-\partial f_0/\partial\mathcal{E})\approx\delta(\mathcal{E}-\mathcal{E}_F)$, where $\mathcal{E}_F$ is the Fermi energy. Hot-spot scattering is included in (3.3) by assuming that $\mathcal{Q}(\mathbf{k},\mathbf{k}')$ has the form

$$\mathcal{Q}(\mathbf{k},\mathbf{k}')=\mathcal{Q}_1(|\mathbf{k}-\mathbf{k}'|)+\mathcal{Q}_2(\mathbf{k},\mathbf{k}'), \quad (3.5)$$

[21] J. M. Ziman, *Principles of the Theory of Solids* (Cambridge University Press, Cambridge, 1964), Chap. 7.

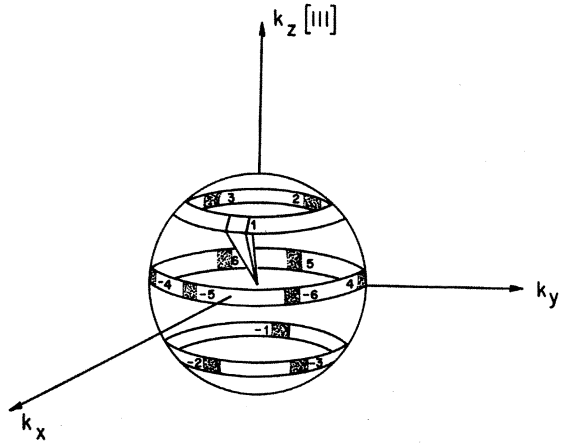

FIG. 4. The geometry of the Fermi surface of $\mathbf{H}\|[111]$. Hot-spot scattering takes place between the ith and $-i$th hot spots.

where $\mathcal{Q}_1(|\mathbf{k}-\mathbf{k}'|)$ is a small-angle isotropic scattering function and $\mathcal{Q}_2(\mathbf{k},\mathbf{k}')$ accounts for the anisotropic scattering of the hot spots. If we approximate the effect of $\mathcal{Q}_1(|\mathbf{k}-\mathbf{k}'|)$ by a relaxation time τ, then (3.3) becomes

$$\mathbf{A}\cdot\mathbf{u}+\omega_c\frac{\partial g(\mathbf{k})}{\partial\varphi}=-\frac{g(\mathbf{k})}{\tau}+\int[g(\mathbf{k}')-g(\mathbf{k})]\mathcal{Q}_2(\mathbf{k},\mathbf{k}')d\Omega'. \quad (3.6)$$

For computational convenience we deform the boundaries of the hot-spot regions on the Fermi surface to resemble squares (Fig. 4). Using these new boundaries, we write $\mathcal{Q}_2(\mathbf{k},\mathbf{k}')$ in the separable form

$$\mathcal{Q}_2(\mathbf{k},\mathbf{k}')=B\sum_{i=-6}^{6}L(\mathbf{K}_i,\mathbf{k})L(\mathbf{K}_{-i},\mathbf{k}'), \quad (3.7)$$

where $\mathbf{K}_{-i}=-\mathbf{K}_i$ (Fig. 3). In (3.7), $L(\mathbf{K}_i,\mathbf{k})=1$ if $\mathbf{k}$ lies within the solid angle Ω_0 about $\mathbf{K}_i$ and 0 if $\mathbf{k}$ lies outside Ω_0. B is a positive arbitrary constant.

The solution of (3.6) using (3.7) assumes the following forms in the different regions of the Fermi surface shown in Fig. 4. For $\mathbf{k}$ lying outside of the hot-spot bands

$$g(\mathbf{k})=g_\tau(\mathbf{k})=\frac{\tau[\omega_c\tau A_y-A_x]}{1+(\omega_c\tau)^2}\sin\theta\cos\varphi-\frac{\tau[\omega_c\tau A_x+A_y]}{1+(\omega_c\tau)^2}\sin\theta\sin\varphi-\tau A_z\cos\theta, \quad (3.8)$$

for $\mathbf{k}$ lying in the hot-spot bands but not in a hot spot

$$g(\mathbf{k})=g_\tau(\mathbf{k})+C_{ij}(\theta)\exp(-\varphi/\omega_c\tau), \quad (3.9)$$

and for $\mathbf{k}$ lying in the ith hot spot we have

$$g(\mathbf{k},i)=\tau^*BG_{-i}+g_{\tau^*}(\mathbf{k})+C_i(\theta)\exp(-\varphi/\omega_c\tau^*), \quad (3.10)$$

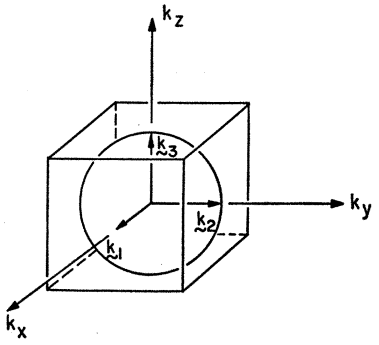

FIG. 5. The Fermi surface and Brillouin zone of a s.c. metal. The anisotropic part of the electron scattering function is a maximum for $\mathbf{k}$ parallel and antiparallel to the $\mathbf{k}_i$'s.

where

$$1/\tau^*=1/\tau+B\Omega_0,$$
$$G_i=\int_{\Omega_0} g(\mathbf{k},i)d\Omega_i. \tag{3.11}$$

The unknown functions $C_i(\theta)$ and $C_{ij}(\theta)$ together with the unknown constants G_i are determined by demanding that $g(\mathbf{k})$ be continuous and periodic in φ.

Using the above solution for $g(\mathbf{k})$ we determine the resistivity tensor from the expression

$$\varrho=(\sigma)^{-1},$$
$$\sigma_{\alpha\beta}=\frac{-3\sigma_0}{4\pi\tau}\int_{4\pi} u_\alpha(\mathbf{k})g_\beta(\mathbf{k})d\Omega \quad (\alpha,\beta=x,y,z), \tag{3.12}$$
$$\sigma_0=\frac{ne^2\tau}{m^*},$$

where $g_\beta(\mathbf{k})$ is the solution of (3.6) when the electric field is in the β direction and n is the number density of conduction electrons.

The parameters B, Ω_0, and τ introduced in the above calculation are easily related to experimental data. If we write the zero-magnetic-field dc resistivity as

$$\rho_{\text{expt}}(\mathbf{H}=0)=m^*/ne^2\tau_{\text{expt}}, \tag{3.13}$$

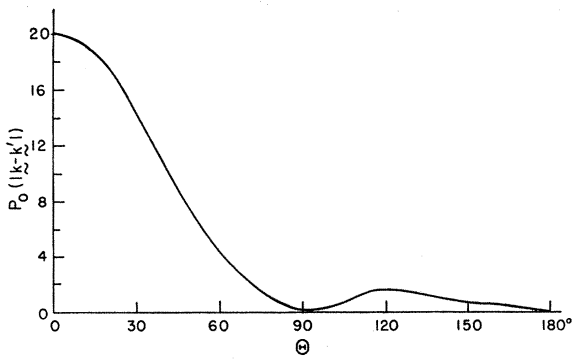

FIG. 6. The anisotropic component of the electron scattering function used in the calculation of the magnetoresistance by the method of JS.

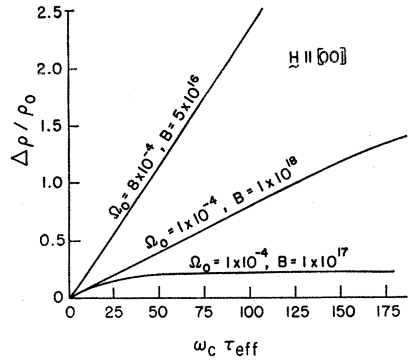

FIG. 7. The average transverse magnetoresistance as a function of $\omega_c\tau_{\text{eff}}$ for $\mathbf{H}\|[001]$. The parameter $\tau\approx\tau_{\text{eff}}=1.4\times10^{-10}$ sec.

then in the case where $\Omega_0\ll1$ it can be shown that $\tau\approx\tau_{\text{expt}}$. If, on the other hand, Ω_0 is not much less than 1, we can calculate an effective relaxation time $\tau_{\text{eff}}(B,\Omega_0,\tau)$ which gives the proper theoretical resistivity and a relationship among B, Ω_0, and τ is determined by requiring that

$$\tau_{\text{eff}}(B,\Omega_0,\tau)=\tau_{\text{expt}}. \tag{3.14}$$

In interpreting the results given in Sec. IV it is to be understood that B, Ω_0, and τ are always related to the zero-field resistivity by means of (3.14).

B. Exact Solution for Large Solid Angle

We expect that as Ω_0 increases the approximation of replacing $\mathcal{Q}_1(|\mathbf{k}-\mathbf{k}'|)$ by a form involving a relaxation time tends to lose much of its validity. That this is true is seen from the fact that as Ω_0 increases, so does the possibility that an electron whose $\mathbf{k}$ vector lies outside a hot-spot region may be scattered into a hot-spot region. Thus although $\mathcal{Q}_1(|\mathbf{k}-\mathbf{k}'|)$ is assumed to give rise only to small-angle scattering, it can cause considerable scattering from regions outside the hot spots to regions inside the hot spots and thus generate large-angle scattering as Ω_0 increases. It is just such two-region scattering that is ignored in the relaxation time

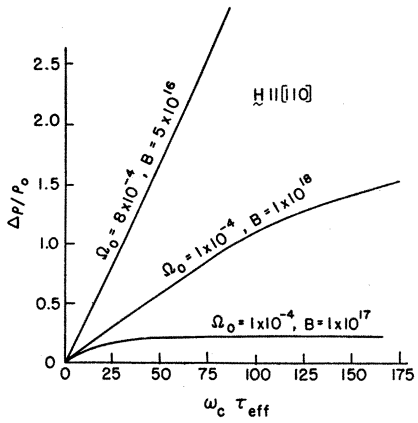

FIG. 8. The average transverse magnetoresistance for $\mathbf{H}\|[110]$. The parameter $\tau\approx\tau_{\text{eff}}=1.4\times10^{-10}$ sec.

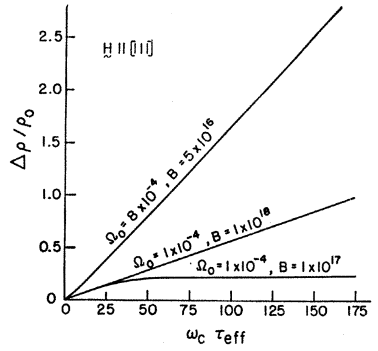

FIG. 9. The average transverse magnetoresistance for H∥[111]. The parameter $\tau \approx \tau_{\text{eff}} = 1.4\times10^{-10}$ sec.

approximation, and the neglect of such scattering could easily affect the quantitative and even the qualitative behavior of the magnetoresistance tensor.

In order to determine just how critical the relaxation-time approximation is to the behavior of the resistivity tensor we have used the method of JS to obtain an exact solution of the Boltzmann equation when we have large anisotropic scattering regions. It is sufficient for our purposes to consider a metal with cubic symmetry and a minimum number of hot-spot regions. For this reason we assume that we have a spherical Fermi surface enclosed by a simple-cubic (s.c.) Brillouin zone (Fig. 5). Although this model does not correspond to our previous one, its resemblance is close enough so that any qualitative difference in the magnetoresistance obtained with the relaxation-time approximation will be evident upon comparison with the exact results obtained with our simpler model. We begin the calculation by rewriting (2.2) of JS in the form

$$\omega_c \frac{\partial g_1}{\partial \varphi} + g_1(\mathbf{k}) \int \mathcal{Q}_0(\mathbf{k}',\mathbf{k}) d\Omega' = -\mathbf{u}\cdot\mathbf{A} + \int \mathcal{Q}_1(\mathbf{k}',\mathbf{k}) g_1(\mathbf{k}') d\Omega', \quad (3.15)$$

where the solution of the Boltzmann equation is given

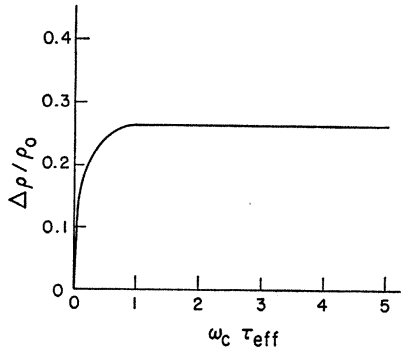

FIG. 10. The average transverse magnetoresistance for H∥[111] and $\Omega_0 \approx \pi/3$, $B = 1\times10^{9}$, $\tau = 1\times10^{-9}$, and $\tau_{\text{eff}} = 1.4\times10^{-10}$ sec. The behavior is typical for H in the other two symmetry directions.

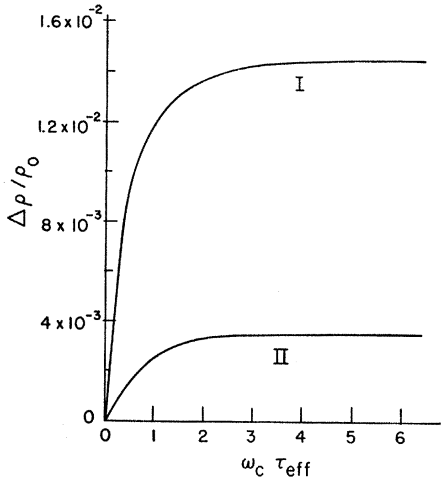

FIG. 11. The average transverse magnetoresistance for a s.c. metal as determined by the method of JS. For curve I the isotropic part of the electron scattering function is zero. For curve II the isotropic part of the scattering function is given by $400(1+\mathbf{k}\cdot\mathbf{k}'/k_F^2)$. For both curves the anisotropic part of the scattering function is that shown in Fig. 6.

by (3.4) and the following notation has been used:

$$g_1(\mathbf{k}) = \tfrac{1}{2}[g(\mathbf{k}) - g(-\mathbf{k})],$$
$$\mathcal{Q}_0(\mathbf{k},\mathbf{k}') = \tfrac{1}{2}[\mathcal{Q}(\mathbf{k},\mathbf{k}') + \mathcal{Q}(\mathbf{k},-\mathbf{k}')], \quad (3.16)$$
$$\mathcal{Q}_1(\mathbf{k},\mathbf{k}') = \tfrac{1}{2}[\mathcal{Q}(\mathbf{k},\mathbf{k}') - \mathcal{Q}(\mathbf{k},-\mathbf{k}')].$$

We choose the following form for $\mathcal{Q}(\mathbf{k},\mathbf{k}')$:

$$\mathcal{Q}(\mathbf{k},\mathbf{k}') = P_0(|\mathbf{k}-\mathbf{k}'|) + \sum_{i=1}^{3} \{P_i(\mathbf{k}')P_i(-\mathbf{k}) + P_i(\mathbf{k})P_i(-\mathbf{k}')\}, \quad (3.17)$$

where

$$P_0(|\mathbf{k}-\mathbf{k}'|) = \sum_{j=0}^{3} c_j[\mathbf{n}(\mathbf{k})\cdot\mathbf{n}(\mathbf{k}')]^j, \quad (3\ 18)$$

$$P_i(\mathbf{k}) = \sum_{j=0}^{3} d_j[\mathbf{n}(\mathbf{k})\cdot\mathbf{n}(\mathbf{k}_i)]^j, \quad (3.19)$$

$\mathbf{n}(\mathbf{k})$ is the unit vector in the $\mathbf{k}$ direction, $\mathbf{k}_i$ $i=1, 2, 3$ are the vectors shown in Fig. 5, and the c_j's are constants. The angular variation of $P_0(|\mathbf{k}-\mathbf{k}'|)$ is shown in Fig. 6

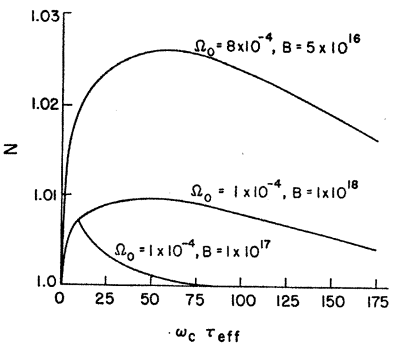

FIG. 12. The variation of $N = (n_e+n_h)/(n_e-n_h)$ for H∥[001]. The behavior is similar for H in the other symmetry directions.

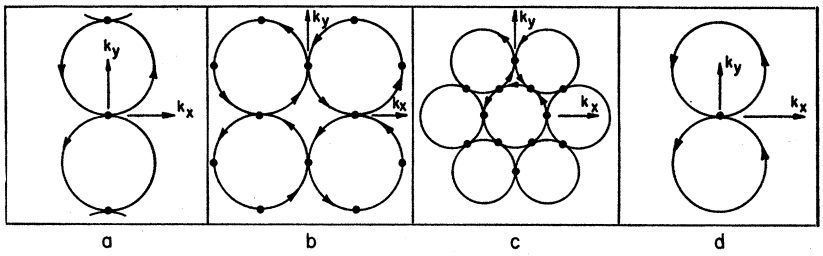

FIG. 13. Projection onto the k_xk_y plane of the electron orbits which pass through hot spots. For H‖[001] orbits of type b occur, for H‖[110] orbits of types a and b occur, for H‖[111] orbits of type c occur, and for H in a nonsymmetry direction orbits of types a and d can occur. The hot spots are indicated by dots.

for a particular set of c_j's. This set is chosen so as to generate the most sharply peaked function of the form (3.18). These same values can be taken for the d_j's to obtain the greatest possible anisotropy in $\mathcal{Q}(\mathbf{k},\mathbf{k}')$. The importance of minimizing the number of hot-spot regions is evident from Fig. 6 since the fewer hot spots the less overlap there is between the functions $P_i(\mathbf{k})$ centered at different $\mathbf{k}_i$. The exact solution of (3.15) using (3.17)–(3.19) is obtained by the method described in Sec. II of JS. The results of this calculation as well as those obtained using the relaxation-time approximation are discussed in Sec. IV.

IV. RESULTS AND DISCUSSION

In Figs. 7–9 we show the results obtained for the transverse magnetoresistance of our bcc model as a function of $\omega_c\tau_{\text{eff}}$ for various orientations of **H**. Figure 10 displays the results for the same model in the case of large Ω_0. Figure 11 shows the results obtained for the simple cubic model using the method of JS and the scattering functions (3.18) and (3.19). In all these figures the value of the ordinate is given by.

$$\frac{\Delta\rho}{\rho_0}=\frac{\frac{1}{2}[\rho_{xx}(\mathbf{H})+\rho_{yy}(\mathbf{H})]-\rho(0)}{\rho(0)}. \tag{4.1}$$

In Fig. 12 we show the behavior of the Hall coefficient for the case **H** parallel to the [001] direction. For this curve the ordinate N is given by

$$N=\frac{[-\rho_{xy}(\mathbf{H})\rho_{yx}(\mathbf{H})]^{1/2}}{\rho(0)\omega_c\tau_{\text{eff}}}, \tag{4.2}$$

which is proportional to the magnitude of the Hall "constant" R.

The most important result of this calculation is the linear magnetoresistance shown in Figs. 7–9. The physical origin of this effect can be seen by considering the following simple model. We assume that for $\Omega_0\ll 1$ we can neglect the dynamics of the electrons inside the hot spots and use instead the approximation that an electron has a probability P of passing undisturbed through the hot spot and a probability Q of suffering umklapp scattering and emerging from the hot spot on the opposite side of the Fermi surface. The probabilities P and Q are magnetic-field dependent (see Appendix). Because we are concerned only with a qualitative explanation of the transverse magnetoresistance, we make the approximation that we can neglect the change of the k_z component of **k** due to hot-spot scattering and that the resultant planar scattering in the k_xk_y plane may be approximated by the two-dimensional models shown in Fig. 13. The conductivity tensor for a group of electrons with hot-spot locations as shown for instance in Fig. 13(b) is easily calculated by the method of Falicov and Sievert.[22] Assuming that a fraction η_1 of the electrons have hot-spot orbits, we then add the conductivity tensor of the fraction $1-\eta_1$ of electrons which experience only a relaxation time scattering over their orbits. The resulting two-dimensional conductivity tensor for large values of $\omega_c\tau$ is given by

$$\boldsymbol{\sigma}=\boldsymbol{\sigma}_{\text{norm}}+\boldsymbol{\sigma}_{\text{hot spot}}$$
$$=\sigma_0\begin{pmatrix}(1+\eta_1X)/(\omega_c\tau)^2 & -(1+Y\eta_1)/\omega_c\tau\\ (1+Y\eta_1)/\omega_c\tau & (1+\eta_1X)/(\omega_c\tau)^2\end{pmatrix}, \tag{4.3}$$

where

$$X\approx\frac{4PQ|\omega_c\tau|}{\pi(P^2+Q^2)} \quad\text{and}\quad Y\approx\frac{2Q[P-(1+Q)]}{\pi(P^2+Q^2)}.$$

If we assume that although $\omega_c\tau\gg 1$ we still have $P\approx\frac{1}{2}$, $Q\approx\frac{1}{2}$ and invert (4.3), we then get

$$\Delta\rho/\rho_0\propto\Omega_0^{1/2}\omega_c\tau. \tag{4.4}$$

Equation (4.4) not only yields a linear transverse magnetoresistance but it also predicts that the slope should vary as $\Omega_0^{1/2}$ when $\Omega_0\ll 1$. This is very close to the dependence found in Figs. 7–9. Using the above model as a guide we can divide the range of magnetic field strengths into three regions as follows: Region 1 is given by $0\leq\omega_c\tau\leq 1$. In this region there is little chance that an electron will be able to traverse the distance separating two successive hot spots without first being scattered back into the equilibrium Fermi sea. Thus, the effect of the hot spots is negligible, and the transverse magnetoresistance increases as $|\mathbf{H}|^2$. Region 2 occurs when $\omega_c\tau\gg 1$ while $P\approx Q\approx\frac{1}{2}$. For this range of magnetic fields the electron is able to pass through many hot spots before being scattered into the equilibrium Fermi sea. In this region we obtain the linear behavior given by (4.4). Region 3 occurs when $\omega_c\tau\gg 1$, and P approaches 1 while Q approaches 0. For this range of magnetic field we can set

$$Q=1-P\approx(\omega_c\tau)^{-1},$$

[22] L. M. Falicov and P. R. Sievert, Phys. Rev. 138, 88 (1965).

where

$$\mathcal{T}=1/B\Omega_0\Delta\,,$$

and Δ is a typical range of the azimuthal angle φ subtended by a hot spot. The insertion of these values into (4.3) yields the saturation of $\Delta\rho/\rho_0$. The saturation value is proportional to $\Omega_0\tau/\tau^*$, where τ^* is given by Eq. (3.11). The results shown in Figs. 7–9 agree remarkably well with the results obtained by the approximate analysis given above. The transition between regions 2 and 3 can be estimated from the formula

$$\omega_c(\text{transition})\mathcal{T}\approx 4$$

if $B\Omega_0\tau\gg 1$.

A further test of the validity of the physical process which gives rise to the linear magnetoresistance can be obtained by considering the behavior of the Hall coefficient as $\omega_c\tau$ increases. The above analysis predicts that in region 2 the Hall coefficient[3] would reach a maximum since $|R|=(|n_e-n_h|\,|e|c)^{-1}$ and the hot-spot scattering generates holelike orbits. From Fig. 12 we see that this increase in R occurs in region 2 as predicted. Since in the intermediate regions, when both hole and electron orbits are present, it is possible to obtain extended orbits or, in the limit, open orbits, the conclusion reached from the above analysis is that these holelike, extended, and open orbits generated by the hot-spot scattering are responsible for the linear magnetoresistance.

The anisotropy of the magnetoresistance shown in Figs. 7–9 is due both to the change in the geometry of the hot-spot orbits (Fig. 13) and the change in the number of electrons undergoing hot-spot scattering as the direction of **H** is varied. For **H** in a nonsymmetry direction it is possible to obtain two different types of hot-spot configurations. One configuration is obtained when **H** is directed so that at least one plane perpendicular to **H** contains more than one hot spot. This arrangement of hot spots can give rise to extended orbits, and we would expect a linear magnetoresistance for these orientations of **H**. A second configuration is obtained when **H** is oriented so that no plane perpendicular to **H** contains more than one hot spot. In this case it is impossible to obtain open orbits [Fig. 13(d)], and we would expect no linear magnetoresistance.

Finally we note that by letting the value of Ω_0 increase up to values ≈ 0.1 we can achieve values of $\Delta\rho/\rho_0\approx 30$ for $\omega_c\tau_{\text{eff}}\approx 150$. It is thus possible to obtain a large variation in the slope of the magnetoresistance by varying Ω_0.

The absence of any linear magnetoresistance at high fields for $\Omega_0\approx\frac{1}{3}\pi$ (Figs. 10 and 11) can also be qualitatively explained using the above model. Since the linear effect is due to the presence of extended and holelike orbits we may expect a linear dependence as long as $P\approx\frac{1}{2}$ and $Q\approx\frac{1}{2}$. The results of Sec. II show that this implies

$$\Omega_0\Delta B/\omega_c\gg 1\,, \tag{4.5}$$

Δ is a typical angle that the electron passes through when traversing a hot-spot region, and B is a transition probability per unit time per unit solid angle. Now for large hot spots we can take $\Omega_0\Delta\approx 1$, so that (4.5) becomes $B/\omega_c\gg 1$. But when the hot-spot region is large, the hot-spot scattering dominates the relaxation time, and we expect that $\tau_{\text{eff}}^{-1}\approx B$ if $B\geq 1/\tau$ and (4.5) finally becomes

$$1/\omega_c\tau_{\text{eff}}\gg 1\,. \tag{4.6}$$

It is clear that (4.6) cannot be satisfied for $\omega_c\tau_{\text{eff}}\gg 1$ and that the linear effect disappears for large Ω_0 as shown in Figs. 10 and 11.

These results dramatically illustrate the inadequacy of any relaxation time approximation when umklapp scattering is not negligible. It is also apparent that such scattering can cause significant deviations from the high-magnetic-field behavior predicted by the LAK theory.

The direct applicability of the above results to any real metal is rather limited due to the ideal model used in studying the problem. Potassium, however, does conform well to the model used in the calculation and, as we have seen, does exhibit the effect of linear magnetoresistance at high fields. The values that the parameters B,Ω_0, and τ must assume in order to obtain a slope similar to the experimental value ($\approx 10^{-3}$) are $B\approx 5\times 10^{18}$, $\Omega_0\approx 1\times 10^{-5}$, and $\tau\approx 1.4\times 10^{-10}$.

It is difficult to attach much physical significance to such a small value of Ω_0 and a large value of B. However, recent experiments by Babiskin[23] show a saturation of the transverse magnetoresistance of polycrystalline potassium for magnetic field strengths between 6 and 15 kG, whereas Penz finds no saturation for field strengths as large as 60 kG. The linear magnetoresistance at very high fields does not appear to be a bulk property of potassium. These results tend to modify the extreme values which Ω_0 and B must assume to fit Penz's data, but the values are such as to make it appear unlikely that hot-spot scattering is totally responsible for the anomalous behavior of potassium. There does exist, however, at least one possible mechanism in potassium which can give rise to sharply localized umklapp scattering and which may also be experimentally observable. It is well known[24] that for transverse phonons with wave vector **q** in the [110] direction there exists a minimum in the sound velocity. Furthermore, the measurements of MacDonald *et al.*[25] show that the resistivity of potassium obeys a T^5 law for temperatures as high as 8°K. The T^5 dependence indicates that the umklapp scattering due to phonons is frozen out over most of the Fermi surface. However, the velocity minimum in the [110] direction could

[23] J. Babiskin (private communication).

[24] See e.g., C. Kittel, *Introduction to Solid State Physics* (John Wiley & Sons, Inc., New York, 1966), 3rd ed., Chap. 4.

[25] D. K. C. MacDonald, G. K. White, and S. B. Woods, Proc. Roy. Soc. (London) **A235**, 358 (1956).

cause a sharp increase in the possibility of umklapp scattering as the electron wave vector $\mathbf{k}$ approaches the [110] direction.

A much more detailed study of the scattering process must be made before one can determine the quantitative effects of scattering by these low-velociy transverse phonons, and the above discussion serves only to indicate that the possibility of highly localized umklapp scattering does exist in potassium.[26] We might also mention that if phonon-generated umklapp processes are responsible for the linear magnetoresistance one should observe a variation in the slope of the magnetoresistance as a function of temperature. On the basis of the above model one would expect that as $T \rightarrow 0$ the effect would disappear and as T increases from zero the slope should reach a maximum and then disappear as $T \rightarrow \Theta_D$ where Θ_D is the Debye temperature for the low-velocity transverse phonons.

Another metal where the above calculation may be qualitatively applicable is aluminum. Although there is new experimental evidence[27] which suggests that much of the anomalous behavior of the magnetoresistance of aluminum is due to magnetic breakdown,[28,29] it is possible that hot-spot scattering at the tips of the arms of the second band hole sheet[30] could enhance the anomalous behavior of the magnetoresistance for field strengths $|\mathbf{H}|$ where the magnetic breakdown probability is small.

Finally, we consider the case of cadmium where recent experiments by Gerritsen and Katyal[31] indicate that hot-spot scattering plays an important role in determining the sign of the Hall resistivity. These experiments confirm that the sign of the Hall resistivity ($\mathbf{H} \| [0001]$) is negative for very low temperatures ($T \approx 1.4°\text{K}$, $H \approx 20$ kG) while for higher temperatures ($T \geq 4°\text{K}$, $H \approx 20$ kG) the Hall resistivity becomes positive. In addition, the temperature at which the Hall resistivity becomes positive is found to increase as the concentration of impurities is increased. This behavior may be qualitatively explained by assuming that the impurities generate hot-spot scattering between adjacent cusps on the "belly" of the second band hole sheet.[32] Such scattering generates electronlike orbits, and the Hall coefficient is negative since the compensation between holes and electrons is thus destroyed. As the temperature increases the increased phonon scattering[12] tends to diminish the effect of this hot-spot scattering and compensation is restored. The geometry of the Fermi surface then causes the Hall coefficient to become positive. A more detailed calculation of the above effect is the subject of other papers.[33]

The metals discussed above serve only to indicate a few of the possibilities for the application of the present theory. In cases where the geometry is simple (potassium) it should be possible to obtain from experimental results the values of the parameters B, Ω_0, and τ. In cases of more complicated geometry (cadmium) the effects of hot-spot scattering may be determined by localizing the scattering to a single point[34] and using the method of Falicov and Sievert[20] together with the expressions for P and Q (see Appendix) to determine the resistivity tensor. In conclusion, it appears that hot-spot scattering does occur in metals and in order to observe its influence on the galvanomagnetic properties one must perform experiments which emphasize scattering and minimize geometric effects, which can often swamp the scattering effects.

ACKNOWLEDGMENTS

The author would like to thank Professor L. M. Falicov for suggesting this problem and for many stimulating discussions. The author would also like to thank Professor M. H. Cohen and Dr. P. A. Penz for valuable discussions. The research benefited from partial support of related solid-state theory by the National Aeronautics and Space Administration and general support of the James Franck Institute by the Advanced Research Projects Agency and the National Science Foundation.

APPENDIX

A. Derivation of Eqs. (2.4) and (2.5)

We begin by dividing time into small intervals δ and letting $t_n = n\delta$. Assuming that the probability per unit time of scattering a particle from $\varphi_{A,i} = \omega_c t_i$ to $\varphi_{B,j} = \omega_c t_j$ is $\mathcal{Q}(\varphi_{B,j}, \varphi_{A,i})$, we find that the probability of scattering out of a state $\varphi_{A,i}$ to any state $\varphi_{B,j}$ during the interval of time δ is given by

$$\sum_{\varphi_{B,j}} \mathcal{Q}(\varphi_{B,j}, \varphi_{A,i})\delta. \tag{A1}$$

Thus the probability that during the time interval $t_{i+1} - t_i$ the particle will propagate to $\varphi_{A,i+1}$ at time t_{i+1} is

$$P_{A,i} = 1 - \sum_{\varphi_{B,j}} \mathcal{Q}(\varphi_{B,j}, \varphi_{A,i})\delta. \tag{A2}$$

Similarly we have for channel B

$$P_{B,i} = 1 - \sum_{\varphi_{A,j}} \mathcal{Q}(\varphi_{A,j}, \varphi_{B,i})\delta. \tag{A3}$$

[26] The presence of a charge density wave has also been proposed as an explanation of the linear magnetoresistance of potassium by J. R. Reitz and A. W. Overhauser, Bull. Am. Phys. Soc. **13**, 42 (1968).

[27] R. J. Balcombe (private communication).

[28] N. W. Ashcroft, Phil. Mag. **8**, 2055 (1963).

[29] V. G. Peschanskii, Zh. Eksperim. i Teor. Fiz. **52**, 1312 (1967) [English transl.: Soviet Phys.—JETP **25**, 872 (1967)].

[30] In aluminum such hot-spot scattering can also cause scattering from the second band hole sheet to the third band electron sheet.

[31] A. N. Gerritsen and O. P. Katyal (private communication).

[32] D. C. Tsui and R. W. Stark, Phys. Rev. Letters **16**, 19 (1966).

[33] O. P. Katyal, A. N. Gerritsen, J. Ruvalds, Richard A. Young, and L. M. Falicov, Phys. Rev. Letters **21**, 694 (1968); Richard A. Young, J. Ruvalds and L. M. Falicov (to be published).

[34] In this approximation the parameters B and Ω_0 no longer have any physical significance. The only significant parameter is $\mathcal{T}$ (see Appendix).

If we now let $W(\varphi_A,t)$ be the probability that the particle will be between φ_A and $\varphi_A+\Delta\varphi_A(\Delta\varphi_A=\omega_c\delta)$ at a time between t and $t+\delta$, the following equations must be satisfied by $W(\varphi_A,t)$ and $W(\varphi_B,t)$:

$$\begin{aligned} W(\varphi_{A,k+1},t_{i+1})&=W(\varphi_{A,k},t_i)P_{A,i}\\ &\quad+\sum_{\varphi_{B,j}} W(\varphi_{B,j},t_i)\mathcal{Q}(\varphi_{A,k+1},\varphi_{B,j})\delta,\\ W(\varphi_{B,k+1},t_{i+1})&=W(\varphi_{B,k},t_i)P_{B,i}\\ &\quad+\sum_{\varphi_{A,j}} W(\varphi_{A\,j},t_i)\mathcal{Q}(\varphi_{B,k+1},\varphi_{A,j})\delta. \end{aligned} \tag{A4}$$

We now let

$$\begin{aligned} W(\varphi_{A,k+1},t_{i+1})&=U(\varphi_{A,k+1},t_{i+1})\Delta\varphi,\\ W(\varphi_{B,k+1},t_{i+1})&=U(\varphi_{B,k+1},t_{i+1})\Delta\Phi. \end{aligned} \tag{A5}$$

Inserting (A2), (A3), and (A5) into (A4), setting $U(\varphi_{A,k+1},t_{i+1})-U(\varphi_{A,k},t_i)=(\partial U_A/\partial\varphi)\Delta\varphi+(\partial U_A/\partial t)\delta$, and taking the limit as $\delta\to 0$, yields

$$\begin{aligned} \omega_c\frac{\partial U_A}{\partial\varphi_A}+\frac{\partial U_A}{\partial t}&=-U_A\sum_{\varphi_{B,j}}\mathcal{Q}(\varphi_{B\,j},\varphi_A)\\ &\quad+\sum_{\varphi_{B,j}} U_B(\varphi_{B,j},t)\mathcal{Q}(\varphi_A,\varphi_{B,j}),\\ \omega_c\frac{\partial U_B}{\partial\varphi_B}+\frac{\partial U_B}{\partial t}&=-U_B\sum_{\varphi_{A,j}}\mathcal{Q}(\varphi_{A,j},\varphi_B)\\ &\quad+\sum_{\varphi_{A,j}} U_A(\varphi_{A,j},t)\mathcal{Q}(\varphi_B,\varphi_{A,j}). \end{aligned} \tag{A6}$$

Finally, we insert $\mathcal{Q}(\varphi',\varphi)=S(\varphi',\varphi)d\varphi'$ in (A6). The resulting equations are identical to (2.4) and (2.5).

B. Derivation of Eq. (2.9)

We add and subtract Eqs. (2.4) and (2.5) to get

$$\begin{aligned} \omega_c\frac{\partial W}{\partial\varphi}+\frac{\partial W}{\partial t}&=-W\int_0^\Delta d\varphi' S(\varphi',\varphi)\\ &\quad+\int_0^\Delta d\varphi' W(\varphi',t)S(\varphi,\varphi'), \end{aligned} \tag{A7}$$

$$\begin{aligned} \omega_c\frac{\partial w}{\partial\varphi}+\frac{\partial w}{\partial t}&=-w\int_0^\Delta d\varphi' S(\varphi',\varphi)\\ &\quad-\int_0^\Delta d\varphi' w(\varphi',t)S(\varphi,\varphi'), \end{aligned} \tag{A8}$$

where we have set

$$W(\varphi,t)=U_A(\varphi,t)+U_B(\varphi,t),\quad w=U_A(\varphi,t)-U_B(\varphi,t),$$

and we have dropped the indices A and B on the variable φ. Eq. (2.7) and (2.8) show that we need not solve (A7) and (A8) directly for W and w but we can integrate (A7) and (A8) over all time and solve the resulting equations in order to determine P and Q. This integration yields

$$\begin{aligned} &\omega_c d\Psi/d\varphi+\{W(\varphi,\infty)-W(\varphi,0)\}\\ &\quad=\Psi\int_0^\Delta d\varphi' S(\varphi',\varphi)+\int_0^\Delta d\varphi' S(\varphi,\varphi')\Psi(\varphi'), \end{aligned} \tag{A9}$$

$$\begin{aligned} &\omega_c d\Gamma/d\varphi+\{w(\varphi,\infty)-w(\varphi,0)\}\\ &\quad=\Gamma\int_0^\Delta d\varphi' S(\varphi',\varphi)-\int_0^\Delta d\varphi' S(\varphi,\varphi')\Gamma(\varphi'), \end{aligned} \tag{A10}$$

where we have set

$$\Psi(\varphi)=\int_0^\infty W(\varphi,t)dt,$$

$$\Gamma(\varphi)=\int_0^\infty w(\varphi,t)dt.$$

Using these definitions the expressions for P and Q are given by

$$\begin{aligned} P&=\tfrac{1}{2}\omega_c[\Psi(\Delta)+\Gamma(\Delta)],\\ Q&=\tfrac{1}{2}\omega_c[\Psi(\Delta)-\Gamma(\Delta)]. \end{aligned} \tag{A11}$$

Since the particle must get through the channel as $t\to\infty$ we can set $W(\varphi,\infty)=w(\varphi,\infty)=0$; also the boundary conditions (2.6) imply $W(\varphi,0)=w(\varphi,0)=\delta(\Phi)$. Since the particle enters channel A at $t=0$, the boundary conditions on Ψ and Γ are

$$\begin{aligned} \Psi(0)&=1/\omega_c,\\ \Gamma(0)&=1/\omega_c; \end{aligned} \tag{A12}$$

thus we must solve the following equations:

$$\begin{aligned} &\omega_c\frac{d\Psi}{d\varphi}-\delta(\varphi)\\ &\quad=-\Psi\int_0^\Delta d\varphi' S(\varphi',\varphi)+\int_0^\Delta d\varphi' S(\varphi,\varphi')\Psi(\varphi'), \end{aligned} \tag{A13}$$

$$\begin{aligned} &\omega_c\frac{d\Gamma}{d\varphi}-\delta(\varphi)\\ &\quad=-\Gamma\int_0^\Delta d\varphi' S(\varphi',\varphi)-\int_0^\Delta d\varphi' S(\varphi,\varphi')\Gamma(\varphi'), \end{aligned} \tag{A14}$$

subject to the boundary conditions (A12). These equations are readily solved by standard techniques when $S(\varphi',\varphi)$ is separable [i.e., $S(\varphi',\varphi)=s(\varphi')s(\varphi)$].

The solution of (A13) for any scattering function is a step function of height $1/\omega_c$; the step occurs at $\varphi=0$.

The solution of (A14) for any separable scattering function is given by

$$\Gamma(\varphi)=D\{e^{-Fu(\varphi)}-(1/2\omega_c F^2)[e^{-Fu(0)}-e^{-Fu(\Delta)}]\}, \tag{A15}$$

$$D=\{\omega_c[e^{-Fu(0)}-(1/2\omega_c F^2)(e^{-Fu(0)}-e^{-Fu(\Delta)})]\}^{-1}, \quad \text{(A16)}$$

$$S(\varphi,\varphi')=s(\varphi)s(\varphi'),$$

$$u(\varphi)=\int s(\varphi)d\varphi,$$

and

$$F=(1/\omega_c)[u(\Delta)-u(0)].$$

In the simplest case, where $s(\varphi)=C^{1/2}$, $0\leq\varphi\leq\Delta$, we find using (A11) that

$$P=\frac{1}{2}\left(1+\frac{e^{-1/\omega_c\mathcal{T}}-\frac{1}{2}\omega_c\mathcal{T}(1-e^{-1/\omega_c\mathcal{T}})}{1-\frac{1}{2}\omega_c\mathcal{T}(1-e^{-1/\omega_c\mathcal{T}})}\right), \quad \text{(A17)}$$

$$Q=1-P,$$

in agreement with Eq. (29).

The fact that $P<\frac{1}{2}$ as $\omega_c\mathcal{T}\to 0$ can be explained as follows. In the case where $C\to\infty$ (i.e., $\omega_c\mathcal{T}\to 0$) the particle is uniformly scattered over a region of width Δ in channel B as soon as it enters the scattering region at $t=0$. During the next increment of time a fraction of this uniform probability density flows out of channel B, the remainder of the density being uniformly scattered back into channel A. During the next increment of time the same process described above occurs in channel A; however, the amount of probability density that flows out of channel A during this second increment of time is less than that which originally flowed out of channel B an instant before. This same periodic process continues as $t\to\infty$. If we now subtract the probability density emerging in channel A from that emerging in channel B in a pairwise fashion it is obvious that $Q-P>0$, and thus that $P<\frac{1}{2}$ as $\omega_c\mathcal{T}\to 0$.

PHYSICAL REVIEW VOLUME 175, NUMBER 3 15 NOVEMBER 1968

Electron-Hole Recombination in Bismuth*

A. A. Lopez
IBM Watson Laboratory, Columbia University, New York, New York 10025
and
Swiss Federal Polytechnic Institute (ETH), Zurich, Switzerland

(Received 29 May 1968)

We have measured the electron-hole recombination time τ_R in bismuth at temperatures from 2 to 50°K for two single-crystal samples with residual resistivity ratios, $\rho_{300°K}/\rho_{4.2°K}$, of 260 and 560. Above ~6°K, the value of τ_R is the same for both samples and decreases rapidly as the temperature increases from $\sim 10^{-8}$ sec at 6°K. We postulate a model in which the absorption or emission of a single phonon provides for momentum conservation in the recombination of electrons and holes. The data above ~6°K can be fitted with two phonons, one of energy (43±4)°K, the other (130±15)°K. We have determined, by group-theoretical methods, the selection rules for the phonons involved, and have shown our data to be consistent with them. At lower temperatures, τ_R becomes a function of sample purity. Below ~3°K, the value of τ_R was found to be temperature-independent for both samples and equal to 1.3×10^{-8} and 2.5×10^{-8} sec, respectively, the ratio of which equals the ratio of the residual resistivities. The results were obtained from measurements of the acoustomagnetoelectric effect (AME) at frequencies ranging from 6 to 35 MHz, in which high-frequency ultrasound sent longitudinally along a sample in a transverse magnetic field generates a dc electric field normal to both the magnetic field and the sound-propagation direction. The dependence of the AME on frequency and on the magnitude and direction of the magnetic field was measured and compared with the theory of Yamada. The temperature dependence of the ultrasonic attenuation coefficient α was also obtained. For $T\leq 20$°K, the attenuation is mainly due to the interaction of the sound wave with carriers via the deformation potential, which interaction also produces the AME. For large magnetic fields, quantum oscillations similar to the de Haas–van Alphen effect are observed in both α and the AME voltage. Electron periods in the trigonal plane are identified. Finally, a lower bound for the deformation potential that describes the change of overlap of the electron and hole bands due to a trigonal compression is obtained: $|E_n-E_p|\geq 1.5$ eV.

I. INTRODUCTION

THE crystal structure of bismuth, a group-V semimetal, is a slight distortion from a simple-cubic Bravais lattice, with two atoms per unit cell.[1] The 10 electrons per unit cell would fill the fifth Brillouin zone were it not for a 0.036-eV overlap[2] with the sixth zone produced by the distortion. The result is a material which, at low temperatures, has 3×10^{17} electrons/cc equally distributed among the geometric-

* Submitted in partial fulfillment of the requirements for a Ph.D. degree at the Swiss Federal Polytechnic Institute (ETH), Zurich.

[1] H. Jones, Proc. Roy. Soc. (London) **A147**, 396 (1934).

[2] D. Weiner, Phys. Rev. **125**, 1226 (1962); N. B. Brandt, T. F. Dolgolenko, and N. N. Stupochenko, Zh. Eksperim. i Teor. Fiz. **45**, 1319 (1963) [English transl.: Soviet Phys.—JETP **18**, 908 (1964)]; G. E. Smith, G. A. Baraff, and I. M. Rowell, Phys. Rev. **135**, A1118 (1964); L. Esaki and P. J. Stiles, Phys. Rev. Letters **14**, 902 (1965); G. A. Williams, Phys. Rev. **139**, A771 (1965); R. N. Bhargava, *ibid.* **156**, 785 (1967). See also Ref. 3.